Nuclear Medicine and Biology 39 (2012) 948–953

Contents lists available at SciVerse ScienceDirect

Nuclear Medicine and Biology

journal homepage: www.elsevier.com/locate/nucmedbio

Comparison of Cerenkov Luminescence Imaging (CLI) and gamma camera imaging for visualization of let-7 expression in lung adenocarcinoma A549 Cells

Weidong Yang [a,1], Weiwei Qin [b,1], Zhenhua Hu [c,1], Yaoyu Suo [a], Rong Zhao [a], Xiaowei Ma [a], Wenhui Ma [b], Tao Wang [d], Jimin Liang [c], Jie Tian [e], Jing Wang [a,*]

[a] Department of Nuclear Medicine, Xijing Hospital, The Fourth Military Medical University, Xi'an, Shaanxi, 710032, China
[b] Department of Hematology, Tangdu Hospital, Fourth Military Medical University, Xi'an, Shaanxi, 710038, China
[c] Life Sciences Research Center, School of Life Sciences and Technology, Xidian University, Xi'an, Shaanxi, 710071, China
[d] State of Key Laboratory of Cancer Biology, Department of Biochemistry, The Fourth Military Medical University, Xi'an, Shaanxi, 710032, China
[e] Institute of Automation, Chinese Academy of Sciences, Beijing 100190, China

ARTICLE INFO

Article history:
Received 29 January 2012
Received in revised form 5 May 2012
Accepted 22 May 2012

Keywords:
miRNA
Cerenkov luminescence imaging (CLI)
Gamma camera imaging
Human sodium/iodine symporter (hNIS)
Let-7

ABSTRACT

Background and Aim: miRNA is an important factor for tumorigenesis which could act as a potential molecular target for tumor diagnosis. The goal of this study was to explore a new method for visualizing the expression of let-7 in lung adenocarcinoma A549 cells by Cerenkov luminescence imaging (CLI) and gamma camera imaging.
Methods: The human sodium/iodine symporter (hNIS) and 3′-UTR sequence of the *ras* gene (RU) that complementarily binds to let-7 were cloned with hNIS serving as the reporter gene. The expression of hNIS regulated by let-7 in the fusion gene hNIS-RU was constructed; the let-7 primer (pri-let-7), which could specifically bind to RU and the mir-143 primer (pri-mir143) not binding with RU, was cloned. A549 cells were transfected with hNIS or hNIS-RU, and additional cells were cotransfected with hNIS-RU and different concentrations of pri-let-7 or pri-mir143. The cells were incubated with 740 kBq ^{131}I-containing media for 1 h, 24 h after transfection. CLI, gamma camera imaging, and γ counting were subsequently conducted, and the correlation among CLI, gamma camera imaging, and γ counting was compared when cotransfected with pri-let-7.
Results: CLI, gamma camera imaging, and radioactive counting showed that hNIS-transfected A549 cells had significantly higher uptake of ^{131}I compared to non-transfected cells. The uptake of ^{131}I in hNIS-RU transfected A549 cells decreased to approximately 70% compared to hNIS-transfected cells, since hNIS-RU expression was suppressed by intracellular let-7. After cotransfection with hNIS-RU and various concentrations of pri-let-7, ^{131}I uptake gradually decreased with increasing pri-let-7, while ^{131}I uptake remained roughly unchanged in the presence of hNIS-RU cotransfected with different amounts of pri-mir143. CLI was highly correlated with gamma camera imaging ($r^2 = 0.9893$) and radioactivity counting (0.9779).
Conclusions: Based upon miRNA-regulated reporter genes which mediate the uptake of the radionuclide, both CLI and gamma camera imaging can noninvasively detect miRNA expression in cells, which may provide a new way for the visualization of miRNA expression.

1. Introduction

miRNAs are a family of small non-coding single-stranded RNAs with approximately 21–25 nucleotides. They regulate target gene expression by directly shearing or inhibiting the translation procedure of the gene after complementary binding to the 3′-untranslated region (3′-UTR) of the gene [1–3], and are involved in multiple biological processes such as early development, cell differentiation, proliferation and apoptosis [4–7]. miRNAs are closely associated with tumorigenesis and are abnormally expressed in tumor tissues serving as oncogenes or anti-oncogenes [8–17]. For example, let-7, whose expression is markedly downregulated in pulmonary carcinoma or breast cancer tissues, can complementarily bind to the 3′-UTR of the *ras* gene to inhibit translation of the gene to the *ras* protein [18–20]. Therefore, miRNA can be considered a novel tumor biomarker, which contributes to the diagnosis of tumors by imaging its expression in tumor cells and tissues.

Commonly used methods for miRNA measurement include Northern hybridization, quantitative RT-PCR, and a miRNA array, all of which do not display *in vivo* miRNA expression [21,22]. The development of molecular imaging has made the visualization of miRNA possible. Through a reporter gene regulated by miRNA, miRNA can be visualized using several substances such as green fluorescent

* Corresponding author. Tel.: +86 029 84775449; fax: +86 029 81230242.
E-mail address: wangjing@fmmu.edu.cn (J. Wang).
[1] These authors contributed equally to this work.

0969-8051/$ – see front matter © 2012 Elsevier Inc. All rights reserved.
doi:10.1016/j.nucmedbio.2012.05.004

protein and luciferase, highlighting the role of optical imaging in miRNA determination [23–25].

Cerenkov luminescence imaging is a kind of optical imaging technique utilizing visible light produced by high-speed charged particles generated during radioactive decay when they pass through the surrounding media. Robertson et al. first performed CLI on mice using positron-emitting radionuclide tracers [26]; since then, CLI has been successfully performed after administration of a radionuclide-labeled probe [27]. Many β emitters, such as ^{18}F, ^{64}Cu, ^{68}Ga, and ^{131}I, can produce Cerenkov light and be used for CLI. Spinelli et al. [28] reported that ^{18}F-FDG was concentrated in the heart and bladder of mice as displayed by CLI when the animals were administered with an agent for optical imaging. Ruggiero et al. [29] demonstrated specific ^{89}Zr-DFO-J591 uptake by tumors using CLI. Therefore, multi-modality imaging can be achieved by combining CLI and radionuclide imaging with a single radionuclide-labeled probe, which provides more comprehensive information. In the present study, the human sodium/iodine symporter (hNIS) which could mediate the uptake of iodine ions could be considered as the reporter gene. In this study, let-7 regulated hNIS which was designed and used for CLI and gamma camera imaging of expressed let-7 in A549 cells in order to establish a new method for miRNA visualization.

2. Material and methods

2.1. Genomic DNA extraction from A549 cells

Genomic DNA was extracted from A549 cells using a mammalian genomic DNA extraction kit (Beyotime, Shanghai, China). Briefly, 1×10^6 A549 cells were centrifuged, and the collected cells were digested at 50 °C with 500 μl protease K containing buffer in a water bath overnight. The sample was double extracted with Tris-phenol, and the remaining water phase was secondarily extracted with an equal volume of chloroform. Ammonium acetate (10 M) and dehydrated ethanol were added to obtain DNA precipitates.

2.2. Construction of a let-7 regulated hNIS reporter gene (hNIS-RU)

The hNIS gene was a gift from Doctor Biao Li of Shanghai Jiaotong Medical University. The let-7 binding *ras* 3′-UTR was cloned and amplified from a template of 1 μl genomic DNA by PCR. The EcoRI-containing upstream primer was sequenced as 5′-ACGAATTCCCTG-GAGGAGAAGTTCCTGT, and the XhoI-containing the downstream primer was sequenced as 5′-ACCTCGAGCTTCTTAAGGTATTCAAAGAA. Twenty-five μl of the reaction contained 1 μl genomic DNA, 1 μl each of the two amplification primers (10 μmol/l), 12.5 μl of the PCR reaction mixture, and the appropriate volume of distilled water. Amplification was performed at 94 °C for 4 min, and the reaction conditions for each cycle were 94 °C for 30 s, 62 °C for 30 s, and 72 °C for 45 s. The extension was performed for 10 min at the end of 35 reaction cycles. The amplified product was treated with EcoRI and XhoI, and cloned into pcDNA3.1 in combination with HindIII and EcoRI-treated hNIS to construct the let-7 regulated fusion vector, pcDNA- hNIS-RU; however, the let-7 unregulated pcDNA-hNIS was also constructed as a control.

2.3. Construction of pri-let-7 and pri-mir143 expression vectors

To test whether or not the expression of hNIS from reporter gene hNIS-RU could be specifically regulated by let-7, mir-143 with the sequence of “ugagaugaagcacuguagcuc” which couldn't complementarily bind with the sequence of RU was selected as a negative control. To increase the expression of let-7 and mir-143 in A549 cells, pri-let-7 and pri-mir143 expression vectors were constructed as follows: the sequence of pri-let-7 and pri-mir143 was cloned from genomic DNA with corresponding primers. For pri-let-7 the upstream primer was: 5′-ACAAGCTTAGGAGCGGATTCAGATAA; downstream primer was: 5′-ACCT CGAGATCCAGTGTACTTGC; for pri-mir143, the upstream primer was: 5′-ACAAGCTT CCTGGGTGCTCAAATGGCAGG; and the downstream primer was: 5′-ACCTCGAGTCGTGAAGCAGATCGT GGCAC. 25 μl of the reaction mix contained 1 μl genomic DNA, 1 μl each of the two amplification primers (10 μmol/l), 12.5 μl of the PCR reaction mixture, and the appropriate volume of distilled water. Amplification was performed at 94 °C for 4 min, and the reaction conditions for each cycle were 94 °C for 30 s, 62 °C for 30 s, and 72 °C for 45 s. The extension was performed for 10 min at the end of 35 reaction cycles. The amplified product was treated with HindIII and XhoI, and cloned into pcDNA3.1 to construct pcDNA-pri-let-7 and pcDNA-pri-mir143.

2.4. Transfection of the plasmid into A549 cells

Pulmonary carcinoma A549 cells were seeded at a density of 1×10^5 cells/well in a 24-well plate and incubated at 37 °C in 5% CO_2 until they reached a confluence of 70%–80%. Transfection was performed using LipofectAmine™2000 after the cell medium was removed. 1 μg of pcDNA-hNIS or pcDNA-hNIS-RU was mixed with 50 μl serum-free DMEM; 2 μl of LipofectAmine™2000 was also mixed with an additional 50 μl serum-free DMEM. After 5 min of incubation at room temperature, serum-free DMEM supplemented with DNA was mixed with the same medium supplemented with LipofectAmine™2000. The mixture was then added to the cells after a 20 min incubation. In addition, A549 cells were also cotransfected with 0, 0.25, 0.5 or 1 μg pcDNA-pri-let-7 or pcDNA-pri-mir143 in combination with 1 μg pcDNA-hNIS-RU according to the above-mentioned procedure. All transfections were performed three times with triplicate wells.

2.5. Northern blotting

Total RNA from A549 cells cotransfected with 0, 0.25, 0.5 or 1 μg pcDNA-pri-let-7 and 1 μg pcDNA-hNIS-RU was extracted using Trizol (Invitrogen, USA). Twenty μg of total RNA was separated on a denaturing 15% polyacrylamide gel using a TBE buffer, then electro-blotted onto the positively charged nylon membrane (Hybond™-N+, Amersham), and the membranes were UV cross-linked and baked for 30 min at 80 °C. DNA oligonucleotides complementary to let-7 sequences were end-labeled with γ-32P-ATP using T4 polynucleotide kinase (NEB). The membranes were pre-hybridized for 30 min with 20 ml of pre-hybridization buffer in a rotating hybridization oven. Hybridization was carried out at 50 °C in a rotating incubator for 24 h. The membranes were then washed with 2× SSC/0.1% SDS buffer three times at 42 °C and exposed to X-ray film. 5 S rRNA served as the loading control.

2.6. CLI, gamma camera imaging and radioactive counting of cellular uptake of ^{131}I

Various transfected A549 cells or non-transfected A549 cells were incubated with DMEM culture medium for 24 h, the medium was removed completely, cells were rinsed in ice-cold PBS three times, then 740 kBq Na^{131}I containing DMEM medium was provided and incubated for an additional hour. One hour later, ^{131}I-containing medium was removed; the A549 cells contained in 24 well plates were rinsed with PBS three times and subjected to CLI and gamma camera imaging. For CLI, images were taken for 5 min with the Xenogen *In Vivo* Imaging System (IVIS Kinetic, Caliper Life Sciences) without using any filters. Regions of interest (ROI) were drawn over the optical images of radioactive sources, and the average radiance was determined by Living Image 3.2 software (IVIS Kinetic, Caliper Life Sciences). For gamma camera imaging, the images were scanned for 5 min with Symbia T2 from Siemens at 128×128 with the zoom set to 1.67. For each gamma camera scan, ROIs were

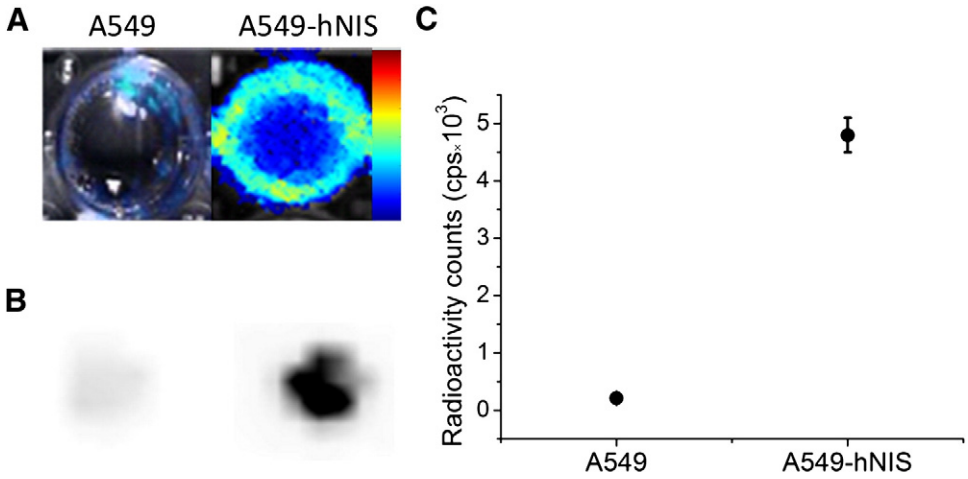

Fig. 1. 740 kBq of $Na^{131}I$ was incubated with the 1×10^5 A549 seeded in 24 well plates, and the expression of the hNIS reporter gene in A549 cells which were transfected with hNIS and non-transfected A549 cells was detected and compared by CLI (A), gamma camera imaging (B), and radioactive counting (C). The uptake of ^{131}I between A549 and hNIS-transfected A549 cells is significantly different ($P<0.001$). Transfections were performed three times with triplicate wells.

drawn over the ^{131}I radiotracer sources to obtain the radioactivity counts. After imaging, cells were collected and used for radioactive counting with a gamma-counter; counting was done in triplicate for each group.

2.7. Statistical analysis

Student *t* test with the *SPSS* 16.0 software was used for statistical analysis. A 95% confidence level was chose to determine the significance between groups, with *P* value of less than 0.05 indicating significant difference. The correlation analyses of Cerenkov luminescence signal with γ camera counts or γ counts was performed using the *Spearman test.*

3. Results

3.1. CLI, gamma camera imaging and radioactive counting of ^{131}I uptake mediated by the hNIS reporter gene

One hour after hNIS-transfected pulmonary carcinoma A549 cells were incubated with ^{131}I, CLI detected clear light signals, which were rarely detected in non-transfected A549 cells (Fig. 1A). The uptake of ^{131}I between A549 and hNIS-transfected A549 cells is significantly different ($P<0.001$), both gamma camera imaging and radioactive counting clearly showed ^{131}I uptake in hNIS-transfected A549 cells, but uptake was almost undetectable in non-transfected A549 cells (Fig. 1B and 1C).

3.2. CLI, gamma camera imaging and radioactive counting of let-7 regulated expression of the hNIS-RU reporter gene

The let-7 presented in A549 cells could complementarily bind to the RU sequence of transfected hNIS-RU to inhibit hNIS expression. Compared to cells transfected with hNIS, CLI, gamma camera imaging and radioactive counting consistently showed that those cells transfected with hNIS-RU had a lower uptake of ^{131}I (Fig. 2A-B), There is significant difference ($P<0.01$) of the uptake of ^{131}I between hNIS-RU and hNIS transefected A549 cells, the uptake of ^{131}I for hNIS-RU transfected cells is approximately 70% of hNIS-transfected cells quantified by radioactive counting (Fig. 2C).

3.3. Differential expression of let-7 in A549 cells detected by CLI, gamma camera imaging and radioactivity counting

After A549 cells were cotransfected with 1 μg pcDNA-hNIS-RU and 0, 0.25, 0.5 or 1 μg pcDNA-pri-let-7, the mature let-7 produced from pcDNA-pri-let-7 inside of the cells could complementarily bind to the RU sequence in the hNIS-RU gene, thereby functioning to inhibit hNIS expression. The study showed that with an increase in pcDNA-pri-let-7, the expression of the let-7 in A549 was dramatically increased (Fig 3A). The escalation of let-7 in A549 cells decreased the uptake of ^{131}I gradually, and the uptake of ^{131}I by cells cotransfected with 1 μg of pcDNA-pri-let-7 was only 50% of the cells that were not

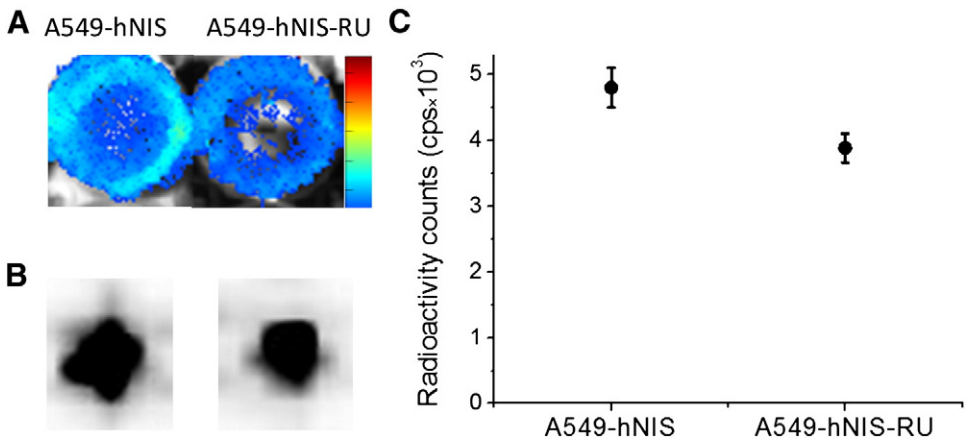

Fig. 2. 740 kBq of $Na^{131}I$ was incubated with 1×10^5 A549 cells transfected with let-7 regulated hNIS (hNIS-RU) or hNIS only in 24 well plates. The expression of let-7 in A549 cells with hNIS-RU and hNIS transfected cells was detected and compared by CLI (A), gamma camera imaging (B), and radioactive counting (C). There is significant difference ($P<0.01$) of the uptake of ^{131}I between hNIS-RU and hNIS transefected A549 cells. Transfections were performed three times with triplicate wells.

cotransfected with pcDNA-pri-let-7 ($P<0.01$, Fig. 3B–D). However, when pcDNA-pri-let-7 was cotransfected with 1 μg pcDNA-hNIS, the increase in the let-7 in A549 did not affect cellular uptake of ^{131}I ($P>0.05$, Fig. 3D). The signal for CLI was highly correlated with that of gamma camera imaging ($r^2=0.9893$, $P<0.001$, Fig. 3E) and radioactivity counting ($r^2=0.9779$, $P<0.001$, Fig. 3 F).

3.4. Specificity of reporter gene hNIS-RU mediated-^{131}I uptake in determining let-7 expression

miRNA can specifically regulate gene expression by complementarily binding with 5-UTR, therefore, mir143 which could not complementarily bind to RU sequence was used as the control. A549 cells were cotransfected with 1 μg pcDNA-hNIS-RU and 0, 0.25, 0.5 or 1 μg pcDNA-pri-mir143, and then subjected to CLI, gamma camera imaging, and radioactive counting to determine their uptake of ^{131}I. In contrast to pcDNA-pri-let-7, increases in cotransfected pcDNA-pri-mir143 did not result in changes in the uptake of ^{131}I, and the images for CLI and gamma camera imaging for the pcDNA-pri-mir143 cotransfected A549 cells were similar to the control cells without pcDNA-pri-mir143 cotransfection (Fig. 4A–B). There was not any significant difference in γ counting between pcDNA-pri-mir143 cotransfected A549 cells and cells without pcDNA-pri-mir143 cotransfection ($P>0.05$, Fig. 4 C).

4. Discussion

In recent years, miRNA has been extensively studied as an important regulatory factor for genes due to its participation in multiple biological processes. It has been revealed that multiple

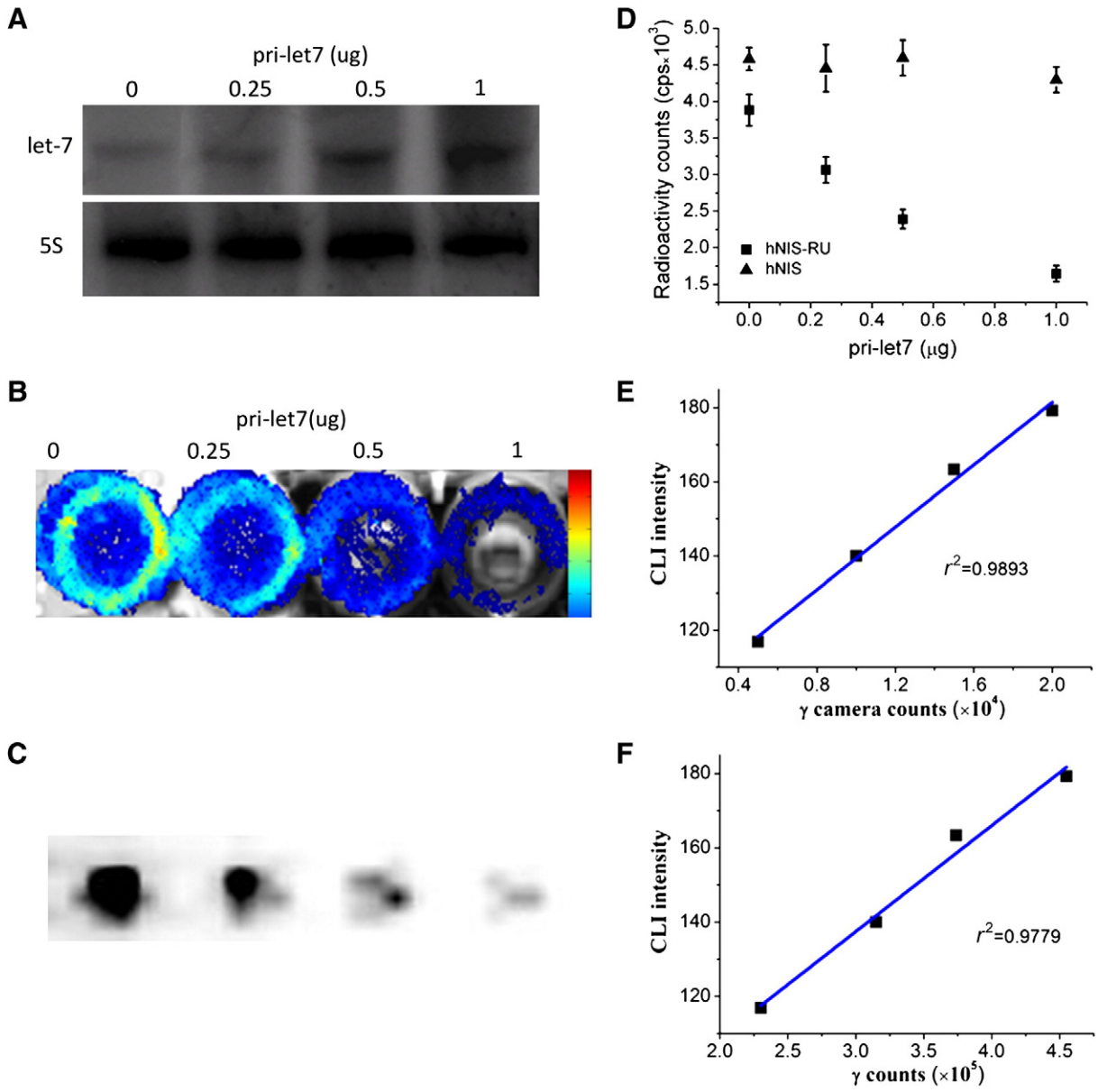

Fig. 3. 740 kBq of $Na^{131}I$ was incubated with the 1×10^5 A549 cells cotransfected with 1 μg hNIS-RU and 0, 0.25, 0.5 or 1 μg pri-let-7. Northern blot of let-7 showed that compared with the endogenous let-7 (first lane), the expression of let-7 in A549 cells was gradually increased with increasing of pri-let-7 transfection (A). The uptake of ^{131}I was decreased with an increase in pri-let-7 which was detected by CLI (B), gamma camera imaging (C), and radioactive counting which showed that the radioiodine uptake decreased with an increase in pri-let-7 when cotransfected with hNIS-RU, the uptake of ^{131}I by cells cotransfected with 1 μg of pcDNA-pri-let-7 is significantly lower than cells that were not cotransfected with pcDNA-pri-let-7 ($P<0.01$), however when pcDNA-pri-let-7 was cotransfected with pcDNA-hNIS, the increase of let-7 in A549 did not affect cellular uptake of ^{131}I ($P>0.05$). (D). The signal for CLI was highly correlated with that of gamma camera imaging ($r^2=0.9893$, $P<0.001$) (E), and radioactivity counting ($r^2=0.9779$, $P<0.001$) (F). Transfections were performed three times with triplicate wells.

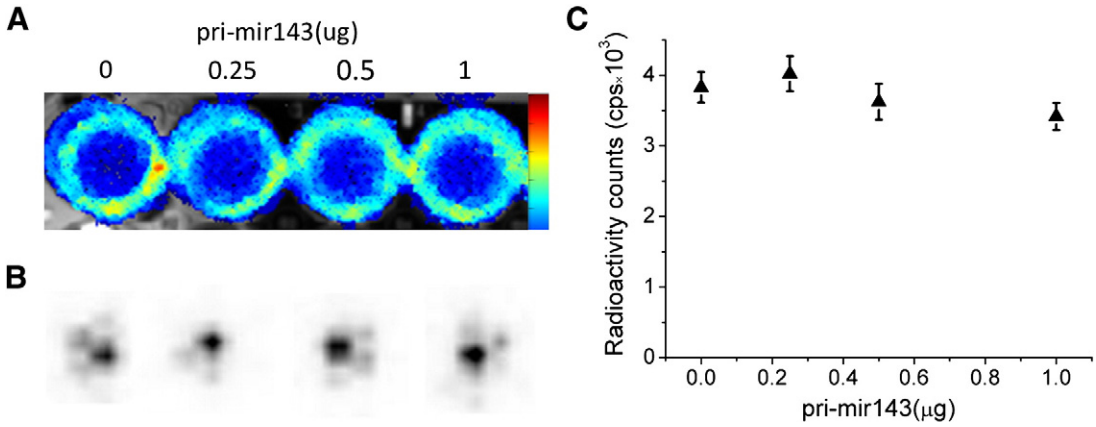

Fig. 4. 740 kBq of $Na^{131}I$ was incubated with 1×10^5 A549 cells cotransfected with 1 μg hNIS-RU and 0, 0.25, 0.5 or 1 μg pri-mir143, and the uptake of ^{131}I remained almost constant with an increase of mir-143 detected by CLI (A), gamma camera imaging (B), and radioactive counting (C). There was not any significant difference in uptake ^{131}I between cells cotransfected pri-mir143 and cells without pri-mir143 cotransfection ($P>0.05$). Transfections were performed three times with triplicate wells.

miRNAs are located in tumor-related genomic domains and serve as oncogenes or anti-oncogenes in close association with the genesis and angiogenesis of tumors [17]. Therefore, abnormally expressed miRNA may be a new target for the diagnosis and treatment of tumors, and determination of miRNA in tumor tissues may be of important significance in understanding the generation and identification of tumors. Since the application of conventional miRNA determination methods such as RT-PCR, Northern hybridization, and miRNA array is limited by their deficiency in *in vivo* miRNA visualization, the fast development of molecular imaging has made the visualization of miRNA possible. Because mRNA can be degraded or inhibited when being translated into protein when miRNA binds completely or partially to the 3′-UTR of the target gene, a miRNA regulated reporter gene can be constructed by connecting a miRNA target sequence to a reporter gene such as a fluorescent protease [30,31]. The expressed miRNA can then be determined based on changes in the reporter gene detected *in vitro* by optical imaging. Currently, the green fluorescent protein, luciferase, and fluorescent nanometer particles were introduced to optical imaging and miRNA as the reporter gene.

Because the hNIS gene can mediate the uptake of the iodine ion or pertechnetate technetium 99 m [32], it has been used extensively in radionuclide imaging as a reporter gene. In the present study, hNIS was considered a reporter gene and connected to the 3′-UTR of the *ras* gene in order to construct the let-7 regulated hNIS-RU fusion gene for reporting purposes, and to evaluate the radioactive counting and radionuclide imaging in determining let-7 expression. It was shown that hNIS could readily uptake ^{131}I. Due to the expression of let-7 in A549 cells, the uptake of ^{131}I in cells transfected with hNIS-RU was significantly lower than that of cells transfected with hNIS alone, suggesting that the hNIS-RU fusion gene was regulated by let-7. Cotransfection with hNIS-RU and pri-let-7, which increased intracellular let-7 levels, additionally reduced the uptake of ^{131}I as manifested by reduced ^{131}I uptake with increasing doses of pri-let-7 (Fig. 3). In contrast, cotransfection with hNIS-RU and pri-mir143 did not affect the uptake of ^{131}I (Fig. 4) because mir143 did not complementarily bind to the RU sequence and inhibit hNIS expression, suggesting specificity of the hNIS-RU fusion gene in determining let-7.

During the beta-decay of ^{131}I, the generated charged high-energy beta particles (606 keV) could produce visible light through Cerenkov radiation when they passed through the surrounding media. In animals, Cerenkov imaging can display the thyroid uptake of ^{131}I after administration of $Na^{131}I$. In the present study, besides visualizing let-7 using hNIS reporter gene-mediated ^{131}I uptake, we also evaluated the determination of let-7 via Cerenkov imaging. The results showed that this technique not only clearly displayed hNIS-mediated uptake of ^{131}I, but also displayed let-7 regulated changes in hNIS (i.e., reduced uptake of ^{131}I in combination with gradually decaying Cerenkov signals due to inhibited hNIS resulting from the up-regulated let-7 expression). The present study also showed a favorable correlation between CLI, gamma camera imaging, and radioactive counting.

In the present study, a visualization and determination procedure for expressed miRNA in tumor cells was established for the first time utilizing radionuclide imaging and CLI, which provides a new direction for miRNA visualization, and also provides a basis for multimodality imaging for the expression of miRNA by combining CLI and radionuclide imaging. However, this issue in the present study should be further investigated using an *in vivo* model based on the cell-based evidence provided here.

In conclusion, as a key regulator of gene expression, miRNA which is abnormally expressed in tumors can be a potential target for imaging. Based on the miRNA-regulated reporter gene-mediated uptake of the radionuclide, both CLI and gamma camera imaging can noninvasively detect the expression of miRNA in tumor cells, which may provide a new way for visualizing miRNA expression.

Acknowledgments

This work was supported by the National Natural Science Foundation of China (Grant Nos. 30970847, 30970846), the Program of the National Basic Research and Development Program of China (Grant No. 2011CB707704), and the Major Program of National Natural Science Foundation of China (Grant No. 81090274).

References

[1] Bartel DP. MicroRNAs: genomics, biogenesis, mechanism, and function. Cell 2004;116:281–97.
[2] Hammond SM, Bernstein E, Beach D, Hannon GJ. An RNA-directed nuclease mediates post-transcriptional gene silencing in Drosophila cells. Nature 2000;404:293–6.
[3] Bartel DP. MicroRNAs: target recognition and regulatory functions. Cell 2009;136:215–33.
[4] Kloosterman WP, Plasterk RH. The diverse functions of microRNAs in animal development and disease. Dev Cell 2006;11:441–50.
[5] Gangaraju VK, Lin H. MicroRNAs: key regulators of stem cells. Nat Rev Mol Cell Biol 2009;10:116–25.
[6] Brennecke J, Hipfner DR, Stark A, Russell RB, Cohen SM. Bantam encodes a developmentally regulated microRNA that controls cell proliferation and regulates the proapoptotic gene hid in Drosophila. Cell 2003;113:25–36.
[7] Xu P, Vernooy SY, Guo M, Hay BA. The Drosophila microRNA Mir-14 suppresses cell death and is required for normal fat metabolism. Curr Biol 2003;13:790–5.
[8] Volinia S, Calin GA, Liu CG, Ambs S, Cimmino A, Petrocca F, et al. A microRNA expression signature of human solid tumors defines cancer gene targets. Proc Natl Acad Sci USA 2006;103:2257–61.
[9] Lu J, Getz G, Miska EA, Alvarez-Saavedra E, Lamb J, Peck D, et al. MicroRNA expression profiles classify human cancers. Nature 2005;435:834–8.

[10] Calin GA, Ferracin M, Cimmino A, Di Leva G, Shimizu M, Wojcik SE, et al. A microRNA signature associated with prognosis and progression in chronic lymphocytic leukemia. N Engl J Med 2005;353:1793–801.
[11] Schetter AJ, Leung SY, Sohn JJ, Zanetti KA, Bowman ED, Yanaihara N, et al. MicroRNA expression profiles associated with prognosis and therapeutic outcome in colon adenocarcinoma. JAMA 2008;299:425–36.
[12] Gabriely G, Wurdinger T, Kesari S, Esau CC, Burchard J, Linsley PS, et al. MicroRNA 21 promotes glioma invasion by targeting matrix metalloproteinase regulators. Mol Cell Biol 2008;28:5369–80.
[13] Si ML, Zhu S, Wu H, Lu Z, Wu F, Mo YY. miR-21-mediated tumor growth. Oncogene 2007;26:2799–803.
[14] Costinean S, Zanesi N, Pekarsky Y, Tili E, Volinia S, Heerema N, et al. Pre-B cell proliferation and lymphoblastic leukemia/high-grade lymphoma in E(mu)-miR155 transgenic mice. Proc Natl Acad Sci USA 2006;103:7024–9.
[15] Voorhoeve PM, le Sage C, Schrier M, Gillis AJ, Stoop H, Nagel R, et al. A genetic screen implicates miRNA-372 and miRNA-373 as oncogenes in testicular germ cell tumors. Cell 2006;124:1169–81.
[16] Ma L, Teruya-Feldstein J, Weinberg RA. Tumour invasion and metastasis initiated by microRNA-10b in breast cancer. Nature 2007;449:682–8.
[17] Zhang B, Pan X, Cobb GP, Anderson TA. microRNAs as oncogenes and tumor suppressors. Dev Biol 2007;302:1–12.
[18] Johnson SM, Grosshans H, Shingara J, Byrom M, Jarvis R, Cheng A, et al. RAS is regulated by the let-7 microRNA family. Cell 2005;120:635–47.
[19] Yu F, Yao H, Zhu P, Zhang X, Pan Q, Gong C, et al. let-7 regulates self renewal and tumorigenicity of breast cancer cells. Cell 2007;131:1109–23.
[20] Kumar MS, Erkeland SJ, Pester RE, Chen CY, Ebert MS, Sharp PA, et al. Suppression of non-small cell lung tumor development by the let-7 microRNA family. Proc Natl Acad Sci USA 2008;105:3903–8.
[21] Iorio MV, Ferracin M, Liu CG, Veronese A, Spizzo R, Sabbioni S, et al. MicroRNA gene expression deregulation in human breast cancer. Cancer Res 2005;65:7065–70.
[22] Lagos-Quintana M, Rauhut R, Lendeckel W, Tuschl T. Identification of novel genes coding for small expressed RNAs. Science 2001;294:853–8.
[23] Brown BD, Venneri MA, Zingale A, Sergi L, Naldini L. Endogenous microRNA regulation suppresses transgene expression in hematopoietic lineages and enables stable gene transfer. Nat Med 2006;12:585–91.
[24] Brown BD, Gentner B, Cantore A, Colleoni S, Amendola M, Zingale A, et al. Endogenous microRNA can be broadly exploited to regulate transgene expression according to tissue, lineage and differentiation state. Nat Biotechnol 2007;25:1457–67.
[25] Kim HJ, Chung JK, Hwang do W, Lee DS, Kim S. In vivo imaging of miR-221 biogenesis in papillary thyroid carcinoma. Mol Imaging Biol 2009;11:71–8.
[26] Robertson R, Germanos MS, Li C. Optical imaging of Cerenkov light generation from positron-emitting radiotracers. Phys Med Biol 2009;54:355–65.
[27] Liu H, Ren G, Miao Z, Zhang X, Tang X, Han P, et al. Molecular optical imaging with radioactive probes. PLoS One 2010;5:e9470.
[28] Spinelli E, D'Ambrosio D, Calderan L, Marengo M, Sbarbati A, Boschi F. Cerenkov radiation allows in vivo optical imaging of positron emitting radiotracers. Phys Med Biol 2001;55:483–95.
[29] Ruggiero A, Holland JP, Lewis JS, Grimm J. Cerenkov luminescence imaging of medical isotopes. J Nucl Med 2010;51:1123–30.
[30] Kato Y, Miyaki S, Yokoyama S, Omori S, Inoue A, Horiuchi M, et al. Real-time functional imaging for monitoring miR-133 during myogenic differentiation. Int J Biochem Cell Biol 2009;41:2225–31.
[31] Lee JY, Kim S, Hwang do W, Jeong JM, Chung JK, Lee MC, et al. Development of a dual-luciferase reporter system for in vivo visualization of microRNA biogenesis and posttranscriptional regulation. J Nucl Med 2008;49:285–94.
[32] Schipper ML, Riese CG, Seitz S, Weber A, Behe M, Schurrat M, et al. Efficacy of 99mTc pertechnetate and 131I radioisotope therapy in sodium/iodide symporter (NIS)-expressing neuroendocrine tumors in vivo. Eur J Nucl Med Mol Imaging 2007;34:638–50.